Water Practice & Technology

IWA PUBLISHING

Water Practice & Technology Vol 18 No 8, 1938 doi: 10.2166/wpt.2023.115

Fenton and solar Fenton processes: inexpensive green technologies for the decontamination of wastewater from toxic Rhodamine B dye pollutant

Padinchare Veettil Gayathri[a,b], Shijo Joseph[a,*], Suguna Yesodharan[c] and E. P. Yesodharan[c]

[a] Department of Climate Variability and Aquatic Ecosystems, Kerala University of Fisheries and Ocean Studies, Puduveype Campus, Kochi 682508, India
[b] Department of Chemistry, St. Albert's College, Kochi 682018, India
[c] School of Environmental Studies, Cochin University of Science and Technology, Kochi 682022, India
*Corresponding author. E-mail: shijonrsa@gmail.com

ABSTRACT

Advanced oxidation processes (AOPs) are projected as relatively cleaner technologies for the abatement of water pollution. This paper investigates the Fenton process as a potential tool for the degradation and eventual mineralization of a textile dye, Rhodamine B (RhB), in water. The effects of activation sources such as microwave (MW), ultrasound (US), and solar energy (SL) on the efficiency of the process were tested. Solar and solar catalytic Fenton processes are identified as the best processes and accordingly, relevant reaction parameters are identified and optimized. The optimum ratio of Fe^{2+}:H_2O_2 obtained is 1:3 at 15 mg/l of RhB concentration and at pH 3–3.5, showing a degradation efficiency of 47% within 30 min of solar irradiation. ZnO enhanced solar Fenton mineralization of RhB. Persulfate (PS) enhances degradation moderately. The study demonstrated the potential of recycling Fe^{2+} by periodic replenishment of H_2O_2. Major reaction intermediates formed were identified by the LC-MS method. Photoluminescence (PL) spectral studies showed a progressive increase in •OH radical formation during solar irradiation. The study has proven that solar Fenton and solar catalytic Fenton processes are efficient AOPs for the complete mineralization of RhB and thus present an economic and environment-friendly technology to remove recalcitrant RhB pollutants from water.

Key words: advanced oxidation process, Fenton reaction, MW Fenton, Rhodamine B, solar Fenton, US Fenton

HIGHLIGHTS

- Solar Fenton and solar photocatalytic Fenton processes are identified as efficient treatment processes for the complete removal of dye pollutants.
- The presence of ZnO as the catalyst enhanced Fenton-assisted mineralization of RhB under solar irradiation.
- The recycling of Fe^{2+} by periodic replenishment of H_2O_2 offers an environment-friendly solution to the accumulation of iron in the waste sludge.

GRAPHICAL ABSTRACT

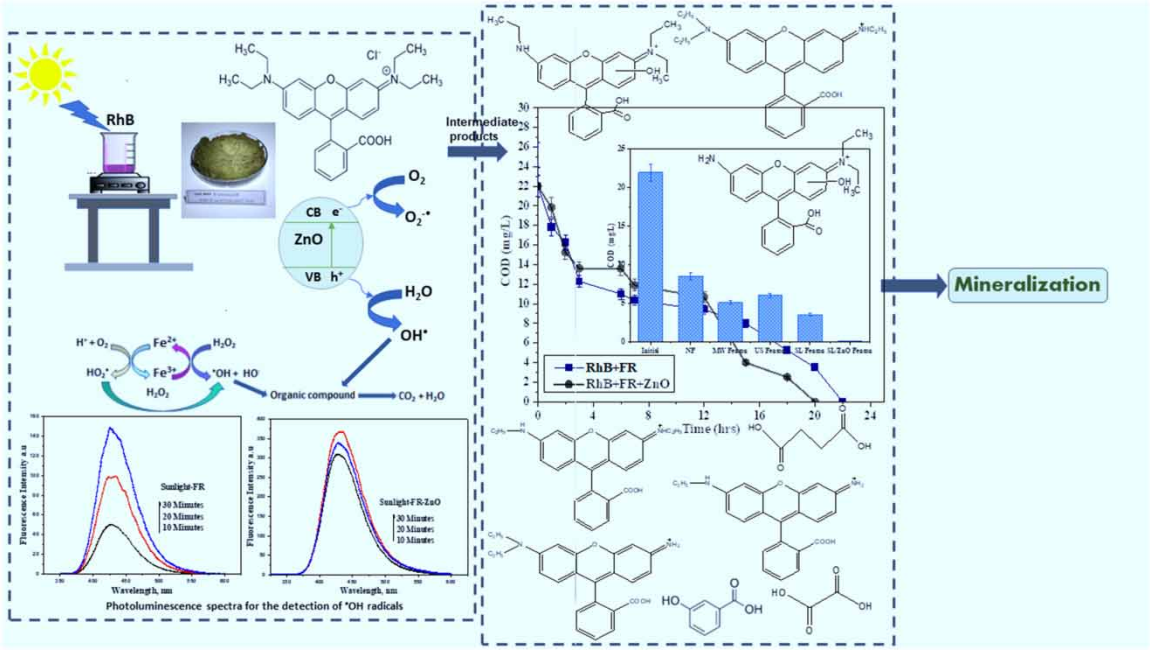

INTRODUCTION

The generation of extremely reactive •OH radicals by the advanced oxidation processes (AOPs) like photocatalysis, sonocatalysis, microwave (MW) catalysis, the Fenton process, and their combinations causes the mineralization of organic contaminants to CO_2, water, and salts (Hoffmann *et al.* 1995; Andreozzi *et al.* 1999; Suty *et al.* 2004; Lu 2013; Ameta & Ameta 2018; Elmobarak *et al.* 2021). Fenton-based AOPs are classified into homogeneous and heterogeneous types depending on the reactive phase. Classic Fenton ($H_2O_2 + Fe^{2+}$), Fenton-like processes ($Fe^{2+} + H_2O_2 + Metal^{n+}$), sono-, photo-, electro-Fenton processes, and other Fenton processes based on O_3, H_2O_2, O_3-UV, H_2O_2-UV, and O_3-H_2O_2-UV, and so on are homogeneous AOPs. Processes involving suspended catalysts belong to the category of heterogeneous AOPs (Ndamitso *et al.* 2020; Onu *et al.* 2023). Reactant molecules get adsorbed at the active sites on the surface of the catalyst and the products get desorbed after the reaction. The use of FeS_2/SiO_2, $(FeTiO_3)/TiO_2$, titanomagnetite (Fe_3TiO_4), etc. as heterogeneous Fenton catalysts was also reported widely (Costa *et al.* 2008; Sivakumar *et al.* 2013; He *et al.* 2016; Diao *et al.* 2017; Luo *et al.* 2021). In the heterogeneous Fenton catalysts, ZnO has received high degree of attention since they are non-toxic, stable, inexpensive, and having high photosensitivity and oxidation capacities. ZnO has a flat band structure (3.35 eV approximately), has spectral overlap with solar emission (about 5%), and is easily applicable in ambient as well as harsh environments. It possesses a relatively large bandgap and offers several positively charged sites for scavenging photo-generated electrons. This prevents their recombination with the holes and promotes redox reactions.

Wastewater treatment using the Fenton process results in improved biodegradability, reduction of toxicity, and/or complete mineralization of the pollutant (Scaria *et al.* 2021; Vilela *et al.* 2021). In the classic Fenton process, when ferrous iron and H_2O_2 are combined, Fe^{2+} ions catalyze the decomposition of H_2O_2 to produce reactive •OH radicals under acidic conditions. The highly reactive species •OH radicals (oxidation potential 2.8 V) can attack organic molecules and lead to their mineralization through the formation of intermediates with rate constants in the range of 10^6–10^{10} M^{-1} s^{-1} (Andreozzi *et al.* 1999; Khare *et al.* 2021). AOPs, with the possible exception of heterogeneous photocatalysis, have so far received only limited acceptance as viable and efficient techniques for the large-scale purification of wastewater due to the complexity of the process, high cost, and practical limitations. Accelerating the transformation of Fe^{3+}/Fe^{2+} and managing the production of Fenton sludge are crucial for resolving the issues related to the Fenton process. The problem of Fenton sludge formation which is the main reason for its poor acceptance as an environment-friendly technology can be resolved by careful design of the component ratio and repeated recycling of Fe^{2+}. The economic viability, input energy, recycling issues,

stability of the process, etc. shall be taken into account for selecting the actual wastewater treatment process. The design of efficient photocatalytic reactors and modification of catalysts by new techniques, which are strongly relevant in catalyst recovery and controlling agglomeration, are also important research areas that require attention.

Recently, AOPs based on ionizing radiation, MWs, and pulsed plasma methods have also received a lot of attention, albeit their economic viability has not yet been established. The simple, low-cost conventional Fenton reaction has drawn renewed interest in this circumstance (Furia *et al.* 2021; Tang *et al.* 2021). The economic efficiency of the mineralization process by combining the Fenton reaction with other AOPs is being widely investigated. Photo-Fenton, sono-Fenton, MW-Fenton, photoelectro-Fenton, etc. are a few of them (Gou *et al.* 2021; Maroudas *et al.* 2021; Yu & Pei 2021; Li *et al.* 2022; Xia *et al.* 2022). In the classic Fenton process (without external activation), the H_2O_2 very slowly oxidizes ferrous to ferric ions leading to the creation of $^{\bullet}OH$ radicals. In the presence of an external source of activation, this reaction is expected to be accelerated as H_2O_2 breaks down very quickly. This paper presents and discusses the results of the investigations on normal and modified Fenton processes as possible candidates for removing hazardous organics from wastewater.

The effluents from the dyeing industry contain hazardous compounds that are harmful to the environment and human health. RhB, a xanthene dye, (IUPAC name: N-[9-(ortho-carboxyphenyl)-6-(diethylamino)-3H-xanthen-3-ylidine] diethyl ammonium chloride, molecular formula $C_{28}H_{31}N_2O_3Cl$, molecular weight: 479.01 g/mole) is a refractory pollutant widely used in the textile and food industries. It is highly toxic, carcinogenic, and mutagenic to humans as well as other species (Du *et al.* 2022). Hence, dye-containing wastewater needs to be thoroughly treated before being discharged into water bodies (Egbosiuba *et al.* 2020; Uko *et al.* 2022), and removing even the last traces of RhB from water is important for environmental sustainability. The structure of RhB is shown in Figure 1. The effect of various parameters such as the ratio of the Fenton Reagent (FR) (a combination of $FeSO_4/H_2O_2$), operating pH, initial concentration of pollutants, the quantity of FR, presence of a catalyst, etc. on the efficiency of degradation of RhB is evaluated and optimized in the present study. The Fenton process as such and with MW, ultrasound (US), and sunlight (SL) as external activation sources are examined in detail, and their efficiencies are compared.

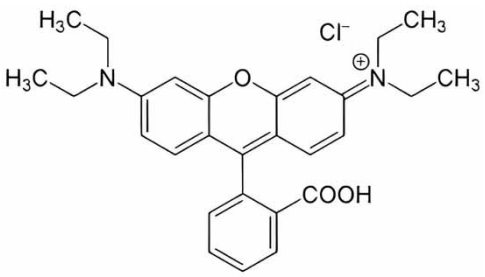

Figure 1 | Structure of Rhodamine B.

MATERIALS AND METHODS

Materials

Rhodamine B (RhB) (>99.6%) and ZnO (>99.5%) were purchased from Sigma Aldrich India and are used as such. H_2O_2 (HP) (30.0% w/v) and $FeSO_4.7H_2O$ (FS) were purchased from Qualigen (India) and used as such without further purification. Unless otherwise stated, other chemicals used were also of AnalaR grade or equivalent.

Experimental setup

The dye solution is combined with the required concentration of FS and HP in a 250-mL closed Pyrex glass reactor in a conventional experiment setup without external activation. The reactor is wrapped in black paper for classic Fenton experiments to prevent any potential photochemical reactions. The solar experiments were carried out on sunny days on the rooftop of our laboratory building in Kochi, Kerala, India. The samples were placed in a 500-mL pyrex glass reactor and at periodic intervals, samples were taken, filtered, and analyzed. An ultrasonic bath (Equitron make) of a frequency of 53-KHz power of 100 W was used for US experiments. By the circulation

of water from a thermostat, the required temperature (29 ± 1 °C) is maintained in the sonicator (10 L). A specially designed jacketed Pyrex glass reactor was used for specific experiments at different temperatures. Experiments using MW radiation were performed in a commercial MW oven (2,450 MHz and 800 W power) modified by making an opening at the top for introducing the reactor. Using a magnetic stirrer, the sample solutions are continuously mixed. The pH of the solution was adjusted to the desired level as needed using 1 N (normal) H_2SO_4 or NaOH.

Methods

An appropriate quantity of the respective aqueous solution (except in the case of the catalyst, which was introduced as solid itself) was added into the RhB solution for experiments with added components, such that the net concentration of the dye, as well as of the additive, would be as desired. In all cases, UV-Vis spectrophotometry at 554 nm was used to monitor the degradation efficiency by analyzing RhB remaining in the solution system. Using standard iodometry methods, H_2O_2 was measured. A fixed amount (0.1 g) of the catalyst in 50 mL of RhB solution in a 250-mL flask was used for adsorption studies (Jain *et al.* 2009; Tijani *et al.* 2022). The pH was adjusted as required for the study. To reach equilibrium, the suspension was constantly stirred for 2 h at a temperature of 29 ± 1 °C. Keeping the suspension overnight before centrifuging had no discernible effect indicating that the 2 h were sufficient to complete the adsorption. Then, it was centrifuged at 3,000 rpm. The colorimetric method was used to measure the concentration of RhB in the centrifugate.

The adsorbate uptake was calculated (Mei *et al.* 2019; Zaidi *et al.* 2021) using Equation (1) as,

$$q_e = \frac{(C_0 - C_e)V}{W} \tag{1}$$

where C_0 is the initial adsorbate concentration (mg/L), C_e is the equilibrium adsorbate concentration in the solution (mg/L), V is the volume of the solution (L), W is the mass of the adsorbent (gm), and q_e is the amount adsorbed in mg/g of the adsorbent.

The photoluminescence (PL) technique was used for testing the formation of $^{\bullet}OH$ radicals in the reaction system using terephthalic acid (TPA) as the probe molecule (Sayed *et al.* 2014). Shimadzu model RF-5301 PC fluorescence spectrophotometer was used for recording the spectrum obtained. The COD (chemical oxygen demand) of the samples was determined using the open reflux method (Eaton *et al.* 2005) and calculated using Equation (2). Complete mineralization is the ultimate goal of the process and hence the favored option must be chosen based on mineralization/COD data. The *in situ*-generated intermediates during the solar Fenton (SF) degradation of RhB at 50% degradation of the substrate are evaluated using the LC-MS (Liquid chromatography-mass spectrometry) technique.

$$\text{COD as mg } O_2/\text{L} = \frac{(A - B)\times M\times 8,000}{\text{Volume of the sample}} \tag{2}$$

where A is the Ferrous Ammonium Sulfate (FAS) (mL) used for the blank, B is the FAS (mL) used for the sample, M is the molarity of FAS; 8,000 is the milliequivalent weight of oxygen × 1,000 mL/L.

Thorough studies were conducted to determine the best ratio of two crucial components FS and HP for RhB degradation under various conditions, i.e., normal Fenton with no external activation (NF), and with activation using SL, US, and MW, by keeping the concentration of RhB constant. Thus, by altering one variable and keeping the other constant, the quantity of FS and HP was optimized. The effect of the FS/HP ratio on the efficiency of the Fenton process is investigated and the ratio is optimized. The RhB concentration of 15 mg/L was kept constant. The concentration of HP was increased from 2.5 to 20 mg/L, keeping the concentration of FS constant at 2.5 mg/L. In order to study the effect of FR-pretreated ZnO, the optimized ratio of FR (1:3) solution is vigorously mixed with 200 mg/L ZnO for 60 min. The ZnO is then filtered, and dried at room temperature and the solar degradation experiment is then carried out. FR-pretreated ZnO exhibits higher RhB degradation after 60 min of solar exposure.

The influence of persulfate on the solar degradation of RhB is investigated with and without ZnO. The persulfate doses ranged from 2.5 to 12.5 mg/L. The net concentration of H_2O_2 in the RhB/FR/ZnO (15/2.5:7.5/200 (mg/L)) system was measured following the decolorization of the suspension both in the presence and absence of FR at pH 6.5 and 3.5. Experiments were carried out to determine if the drop in H_2O_2 concentration in the

system containing Fe^{2+} is caused by the latter's rapid interaction with the former during solar irradiation. After decolorization under SL, the quantity of H_2O_2 in sample solutions of RhB + ZnO and RhB + ZnO + FR is measured. Then, each sample solution is separated into two portions. One half (C) receives 2.5 mg/L of Fe^{2+} addition and is exposed to SL for 60 min. The other half (B) is exposed to radiation for 60 min without the addition of Fe^{2+} and the H_2O_2 is calculated.

In the Fenton process, the excess reagent successfully employed to degrade the fresh substrate is tested by progressively adding more FR/HP/FS (1:3/7.5/2.5 mg/L) to a reaction system containing optimized concentrations of pollutant and reagents where the pollutant degradation leveled off due to insufficient reagent. The recycling of Fe^{2+} is done when pollutant degradation in the SF case reached a peak. An extra 7.5 mg/L of H_2O_2 was introduced to the system to efficiently use the remaining FS and fresh RhB (15 mg/L) solution is supplied to the system once the decomposition of the RhB is completed. More H_2O_2 is injected once the degradation has stabilized and more RhB is added when degradation is completed, which is done continually. After initial use, the system's ability to recycle Fe^{2+} is examined by periodically replacing the H_2O_2 that was used up in the FR.

RESULTS AND DISCUSSION

The classic Fenton process and its combination systems were evaluated for the degradation/decolorization/mineralization of RhB. The ratio of FS and HP concentration affects the efficiency of the process. For best removal efficacy, the HP/FS ratio must be at its optimal value. Therefore, the results of the degradation of RhB in the classic Fenton process, and the MW-, US-, and SL activated processes are compared. The optimum concentration of RhB and FR obtained is different for each system and is compared to finding the best system under respective optimized conditions. The best system is identified as the SF process (Figure 2) and the following component ratio is chosen as ideal for further experiments.

- NF: FS/HP = 4:1
- US: FS/HP = 4:3
- MW: FS/HP = 1:4
- SL: FS/HP = 1:3

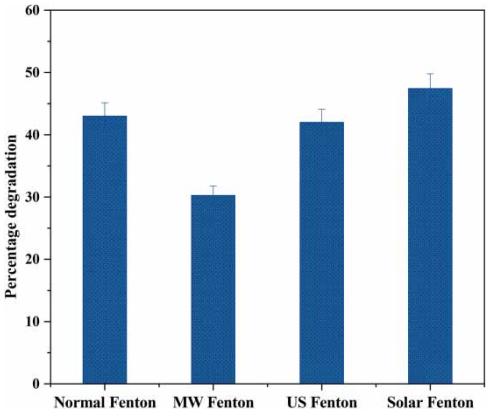

Figure 2 | Comparison of the efficiency of various Fenton processes for the degradation of RhB: Classic Fenton (RhB:15 mg/L + FR ratio 4:1); MW Fenton (RhB:12.5 mg/L + FR ratio 1:4); US Fenton (RhB:12.5 mg/L + FR ratio 4:3); SF (RhB:15 mg/L + FR ratio 1:3); time: 30 min.

The degradation efficiency (47% for SF , 43% for NF, 42% for US Fenton, and 30% for MW Fenton within 30 min of time) at the respective optimum ratio of Fenton components is in the order: SF > NF > US-Fenton > MW-Fenton.

The COD determines the effectiveness of any AOP and in the study COD decreases after decolorization, indicating that at least some of the intermediates are unstable and are getting mineralized. However, the COD does not really alter much after the initial reduction, most likely because some of the intermediates generated might be more resilient and persistent. Even after prolonged hours, the Fenton process does not degrade them. Thus, it can

be concluded that the Fenton process is an effective inexpensive way to decolorize RhB contaminants from water. Complete mineralization, on the other hand, occurs more slowly, suggesting the presence of resistant, slowly degrading intermediates. To accomplish total mineralization in such circumstances, a combination of the Fenton process with external sources of activation like photo, sono, and MW may be needed.

The optimum concentration of RhB obtained is different for each system and is used to compare the COD reduction in order to find the best system under respective optimized conditions (concentration of RhB, FR, and catalyst dosage). The comparative study of the COD reduction under different Fenton-based processes is presented in Figure 3 and the complete COD removal was possible only in the SF and solar catalytic Fenton processes using ZnO as the catalyst. The results demonstrated the superiority of the use of renewable solar energy and ZnO catalyst for effective degradation/mineralization of RhB using the Fenton process. Hence, the SF process is investigated in detail. The COD reduction was used to show the effectiveness of the best system identified, i.e., solar catalytic Fenton process. It was not an exact comparison of the three processes, which may not be meaningful in view of the different optimum values. To the best of our knowledge, this is the first report on the application of the SF process in the presence and absence of ZnO as a catalyst for the removal of RhB dye pollutants in water. This is also the first instance of comparison of the efficacy of different Fenton processes, i.e., classic Fenton, photo-Fenton, MW Fenton, and US Fenton processes for the removal of RhB pollutants from water.

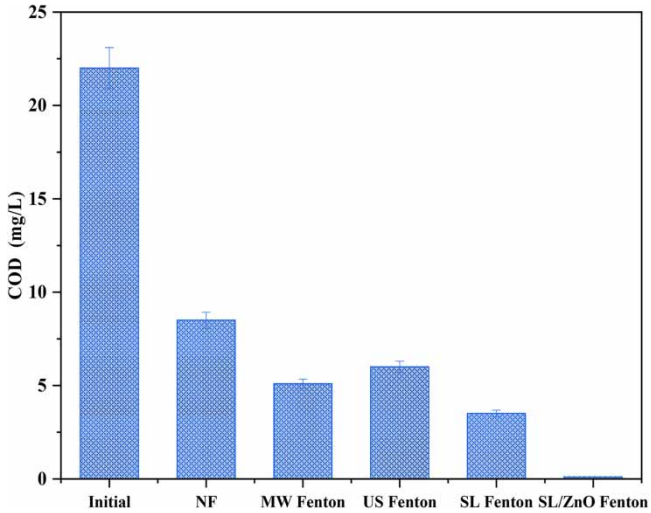

Figure 3 | Comparison of the COD reduction using different Fenton processes: Classic Fenton (RhB:15 mg/L + FR ratio 4:1); MW Fenton (RhB:12.5 mg/L + FR ratio 1:4); US Fenton (RhB:12.5 mg/L + FR ratio 4:3); SF (RhB:15 mg/L + FR ratio 1:3); [ZnO]: 200 mg/L; time: 20 h.

SF process

Combination of Fenton reaction with light as the source of activation, i.e., photo-Fenton is known to enhance the efficiency of the process (Babuponnusami & Muthukumar 2011; Sannino *et al.* 2012; Pouran *et al.* 2015; Çalık & Çifçi 2022). The current study, as reported earlier in this paper, shows that the Fenton process in combination with MW/US activation is not effective for the complete mineralization of RhB pollutants in water while the SL-Fenton combination (SF) gave encouraging results (Figure 3). Hence, the SF process is examined in depth for the degradation/mineralization of RhB pollutants. The efficiency of the Fenton process depends on the relative concentrations of FS and HP (Gulkaya *et al.* 2006; Ghosh *et al.* 2010; Asgari *et al.* 2020). Hence, the ratio of these critical components is optimized initially.

Optimization of FS/HP ratio

The degradation increases with an increase in the quantity of HP (keeping FS constant) but eventually slows down when the ratio of HP/FS is > 3. Thereafter, the rate of degradation does not increase in accordance

with the rise in H_2O_2 concentration (Figure 4). Hence, the optimum ratio of FS/HP is selected as 1:3 (2.5:7.5 (mg/L)).

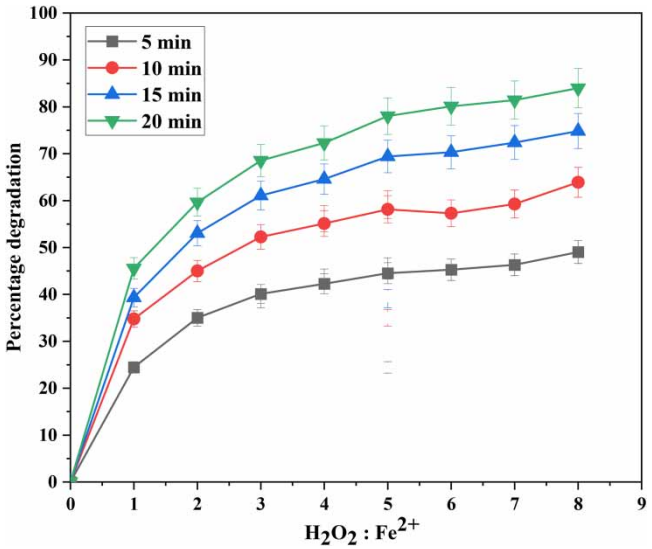

Figure 4 | The effect of H_2O_2/Fe^{2+} ratio on SL/FR/RhB degradation. [RhB]: 10 mg/L; [Fe^{2+}]: 2.5 mg/L.

Effect of the quantity of FR

The optimum dosage of the FR for the degradation of a fixed quantity of RhB under SL is already found at the ratio of FS: HP (1:3). However, the rate of degradation gradually slows down at higher concentrations of FR (above FS: HP = 5:15), even when the ratio of FS: HP is maintained 1:3. This is most likely the result of the dye concentration becoming too low to effectively utilize the increased availability of FR (Figure 5).

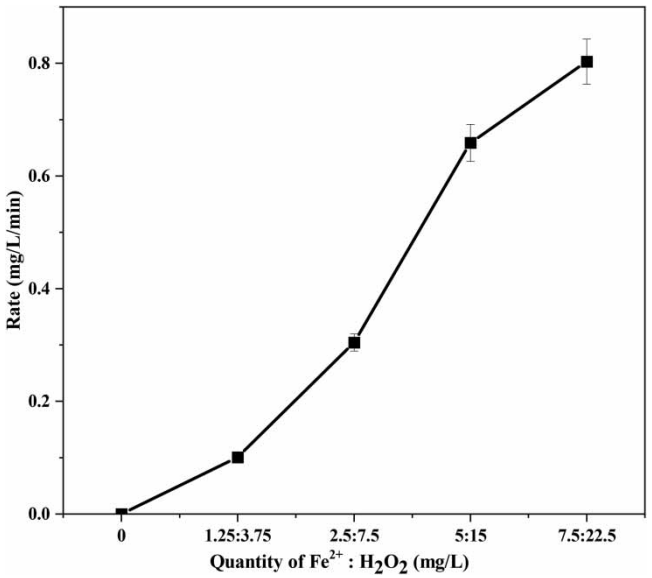

Figure 5 | The effect of quantity of FR on the rate of SL/FR/RhB degradation. [RhB]: 15 mg/L; pH: 4–4.5.

The study of the effect of RhB concentration (5–25 mg/L) on the rate of degradation shows that the rate drops above a particular concentration. Beyond the optimum concentration, the amount of FR that is readily available might not be enough to interact with and degrade all the RhB molecules. At higher dye concentrations (in the range examined here), the reaction system is less effectively activated by solar radiation probably due to its

decreased penetration, which results in a reduction in the generation of ˙OH radicals. When there is enough FR in the solution, the dye will degrade rapidly and with an increase in the concentration of dye, the rate of degradation also rises. However, once the concentration is over the optimal level, the rate of degradation steadily decreases (Figure 6). As a result, 15 mg/L of RhB is selected as ideal for further studies, which had a maximum rate of 0.329.

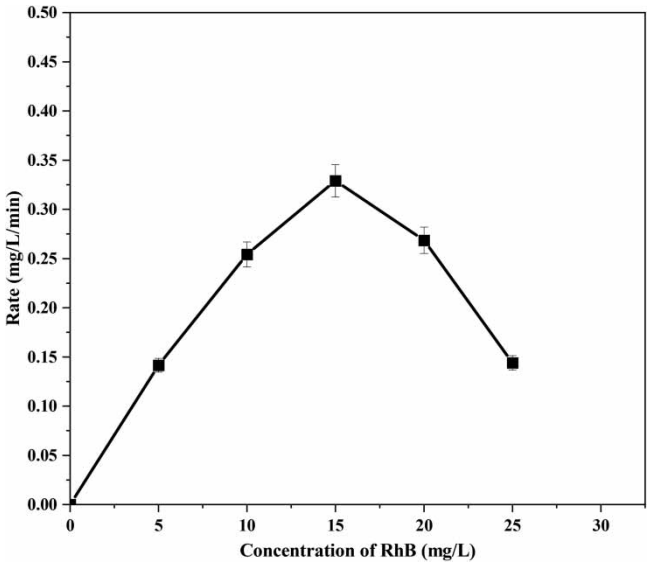

Figure 6 | The effect of RhB concentration on its rate of SL/FR degradation (Fe^{2+}/H_2O_2): (2.5/7.5) mg/L; pH: 3.05.

The interaction between the RhB molecule and the reactive free radicals will be more effective as the concentration of the dye is increased. This leads to an increase in the rate of reaction. Beyond the optimum, the rate of degradation slows down because the relative concentration of ˙OH radicals to interact with all the RhB molecules will be less. This leads to a steady state or even a decrease in the degradation rate. At higher concentrations, the dye molecules are excessively large in comparison to the amount of FR needed for efficient degradation. Since H_2O_2 is primarily responsible for degradation, any hindrance to the ability of H_2O_2 to interact with Fe^{2+} to produce ˙OH radicals will result in a reduction in degradation.

Effect of ZnO

Since the SF process produces more reactive free radicals compared to the NF process, the former is highly effective. The addition of a photoactive semiconductor oxide in this situation may result in concurrent photocatalysis, thereby increasing the probability of RhB degradation. Previous research has demonstrated that photocatalysis mediated by ZnO and TiO_2 is effective for the mineralization and degradation of a variety of contaminants (Anju *et al.* 2012; Jyothi *et al.* 2014; Gayathri *et al.* 2017; Pandey *et al.* 2020; Saeed *et al.* 2021). Due to the superior visible light absorption properties, ZnO has been shown to be the more active of these two extensively researched semiconductor oxides for solar energy harvesting (Babuponnusami & Muthukumar 2011; Gayathri *et al.* 2019; Veena *et al.* 2019; Shah *et al.* 2022). Therefore, by the addition of ZnO to the system, the photo-Fenton process for RhB degradation can be made more effective. It has already been established that ZnO inhibits the degradation in the conventional Fenton process in the absence of light irradiation (Gayathri *et al.* 2016). However, the trend is different in the presence of SL (Figure 7) as a result of the photochemical and photocatalytic properties of ZnO.

ZnO initially inhibits the degradation even in the presence of light. The degradation, however, increases with an increase in reaction time and ZnO concentration as shown in the figure. The solar photocatalytic-Fenton process is more effective than the classic Fenton process. The Fe^{3+} ions generated from the FR ($Fe^{2+}{}^{+}H_2O_2 \rightarrow Fe^{3+} + OH^- + {}^{\bullet}OH$) are more effectively reversed into Fe^{2+} by photoreduction in the presence of light as shown in the following equation (Equation (3)):

$$Fe^{3+} + H_2O + h\nu \rightarrow Fe^{2+} + H^+ + {}^{\bullet}OH \quad (3)$$

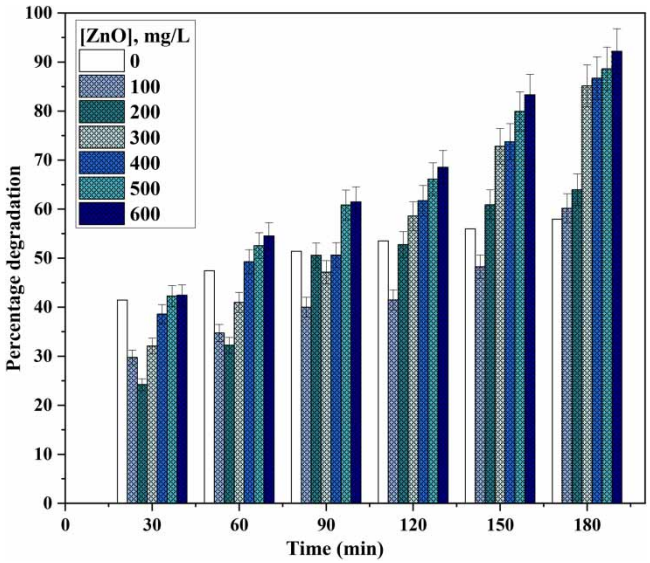

Figure 7 | The effect of ZnO dosage on the SL/FR/RhB degradation [RhB]: 15 mg/L; (Fe^{2+}/H_2O_2): (2.5/7.5) mg/L.

Additionally, it is probable that some H_2O_2 undergoes direct photolysis to produce $^{\bullet}OH$, as in Equation (4). This may also speed up RhB degradation.

$$H_2O_2 + h\nu \rightarrow 2^{\bullet}OH \tag{4}$$

The application of the optimized parameters for the SF process [RhB/(Fe^{2+}:H_2O_2) = 15/(1:3)] for ZnO solar photocatalytic-Fenton too is illustrated in Figure 8. ZnO inhibits RhB degradation in the absence of radiation. However, when the same system is exposed to SL, the ZnO-induced inhibition gradually slows down, and eventually, the degradation is comparable to that of the SF process, which contains no ZnO. Finally, conventional photocatalysis with ZnO (ZnO/SL), also produced the same result. Though the degradation is initially faster in the case of SF, attaining early decolorization, solar photocatalysis, and solar photocatalytic-Fenton become comparable at later stages of the process.

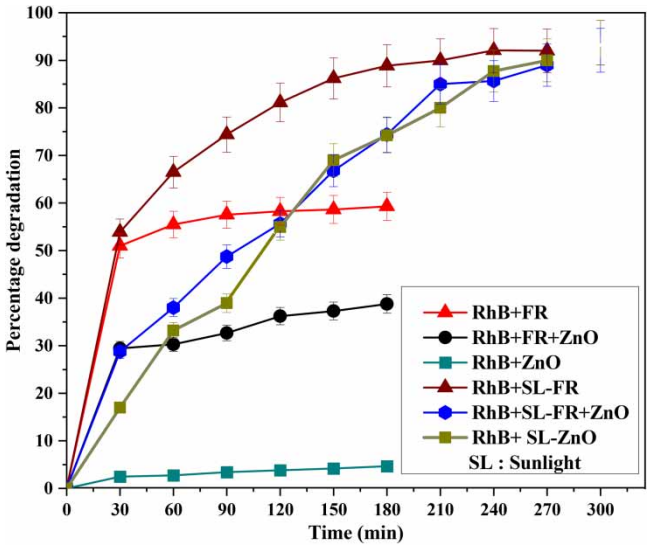

Figure 8 | Effect of ZnO on the efficiency of the SL/FR/RhB degradation under different conditions [RhB]: 15 mg/L; [ZnO]: 200 mg/L; [Fe^{2+}/H_2O_2]: [2.5/7.5] mg/L; pH: 3–3.5.

Effect of pH

It has been established from prior investigations that pH has a critical role in the effectiveness of Fenton processes. Additionally, it has also been shown that ZnO can alter the pH of the RhB/FR system. The degradation of RhB at two different pH ranges (3–4 and 6.5–6.8) is presented in Figure 9. At pH 3, ZnO substantially slows down the initial rate of SF degradation. In the end, though, the inhibition is overcome, and degradation is more when ZnO is present. In both cases, (RhB + ZnO) and (RhB + FR + ZnO), the photocatalytic degradation in the presence of ZnO at pH 6.9 is not significantly influenced by FR. This demonstrates that adding ZnO to the reaction system can reduce the pH sensitivity of the Fenton process. Even though the initial effect of ZnO is inhibition, it also has the ability to accelerate the SF degradation of RhB with time. In any case, solar photocatalysis and solar photocatalytic-Fenton have almost the same decolorization efficiency.

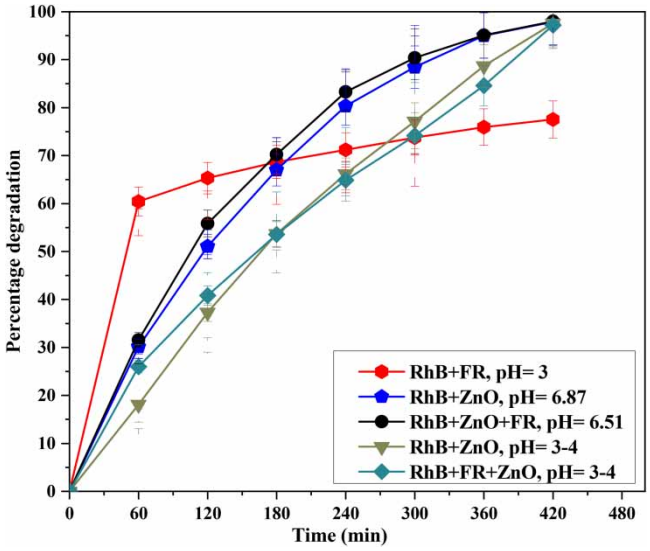

Figure 9 | Effect of ZnO at different pH values on SL/FR/RhB degradation. [RhB]: 15 mg/L; [ZnO]: 200 mg/L; [Fe^{2+}/H_2O_2]: [2.5/7.5] mg/L.

The mineralization of RhB is the most important factor to be taken into account when analyzing the role of ZnO on the efficacy of the Fenton process. The COD of RhB contaminated water under optimized conditions of the SL/Fenton process at different times of solar irradiation with and without ZnO is presented in Figure 10. The COD decreases drastically after decolorization, with or without ZnO, as seen in the figure, showing that at least part of the intermediates created during decolorization is unstable and quickly mineralize. Prolonged Fenton treatment with an appropriate H_2O_2 supply leads to a decline in COD and total mineralization. As a result, it can be established that the photo-Fenton process, and in particular the ZnO photocatalytic-Fenton process is a cost-effective and efficient technique for the total removal and mineralization of RhB contaminants from water.

Formation of H_2O_2

The NF process is one among several AOPs that produce H_2O_2 as a byproduct. H_2O_2 concentration is seen to be lower in solutions containing FR at both pH levels 6.5 and 3.5. The net concentration of H_2O_2 was anticipated to be larger as the FR already contains H_2O_2. H_2O_2 is decomposed by Fe^{2+}, as evidenced by the drop in concentration of H_2O_2 in the presence of FR (Figure 11). It was observed that when additional Fe^{2+} was added to the RhB + ZnO system, the H_2O_2 concentration decreases. The system (RhB + ZnO + FR) is unaffected by the added Fe^{2+} because it already contains Fe^{2+}. This indicates that Fe^{2+} interacts with and decomposes H_2O_2.

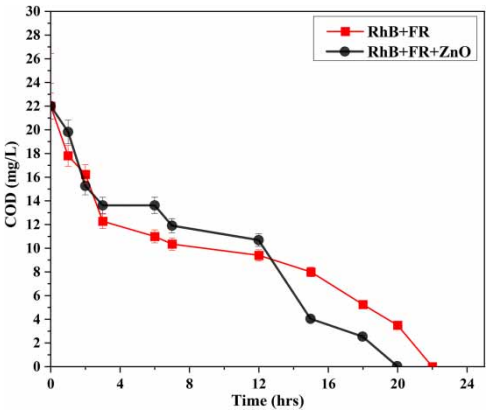

Figure 10 | Complete removal of COD in SL/FR/RhB/ZnO and SL/FR/RhB systems [RhB]: 15 mg/L; [Fe^{2+}/H_2O_2]: [2.5/7.5] mg/L; [ZnO]: 200 mg/L.

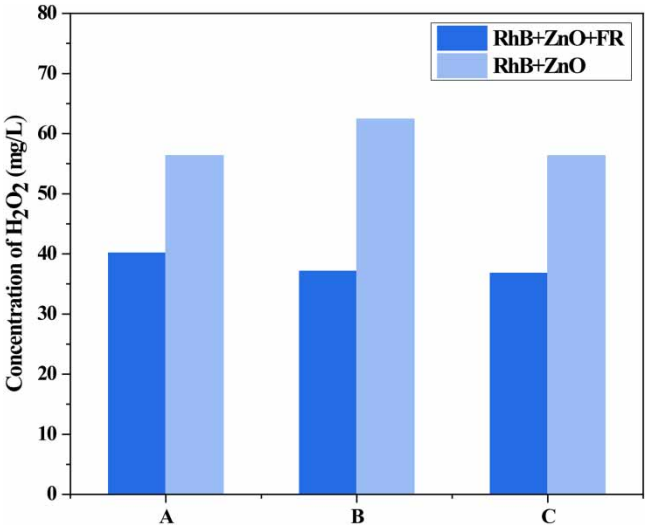

Figure 11 | Measurement of the H_2O_2 concentration in RhB/FR/ZnO systems following exposure to SL in the presence and absence of additional Fe^{2+}. (A) Decolorized sample solution, (B) decolorized sample solution after 1 h of solar exposure, (C) decolorized sample solution with additional Fe^{2+} and 1 h of solar exposure. [RhB]: 15 mg/L; [Fe^{2+}/H_2O_2]: [2.5/7.5] mg/L; [ZnO]: 200 mg/L; [Fe^{2+}(extra)]: 2.5 mg/L.

Effect of FR-pretreated ZnO

It has already been established from earlier investigations (Gayathri *et al.* 2017; Kondamareddy *et al.* 2018) that RhB adsorption on ZnO is minimal. The possibility of FR adsorption on ZnO as the cause of the initial inhibition is explored because FR/ZnO showed enhancement in RhB degradation in the presence of SL after initial inhibition. The FR pretreated ZnO exhibits a higher RhB degradation after 60 min of solar exposure (Figure 12).

The trend indicates that in the presence of ZnO, the solar degradation of RhB (photocatalysis) will continue and finally approach the same degradation as in the presence of FR/SL. RhB degraded more rapidly in FR-pretreated ZnO. This suggests that inhibition (by ZnO) of classic Fenton degradation of RhB may be at least partially due to the adsorption of FR over ZnO.

Effect of persulfate on the SL/FR/RhB degradation

Due to the generation of extremely reactive $SO_4^{-\bullet}$ radical anions, persulfates have been proven to be powerful oxidants in AOPs (Norzaee *et al.* 2017; Venâncio *et al.* 2022). The influence of persulfate on the solar degradation of RhB indicated that persulfate has a positive influence on degradation, most likely as a result of efficient $SO_4^{-\bullet}$ production.

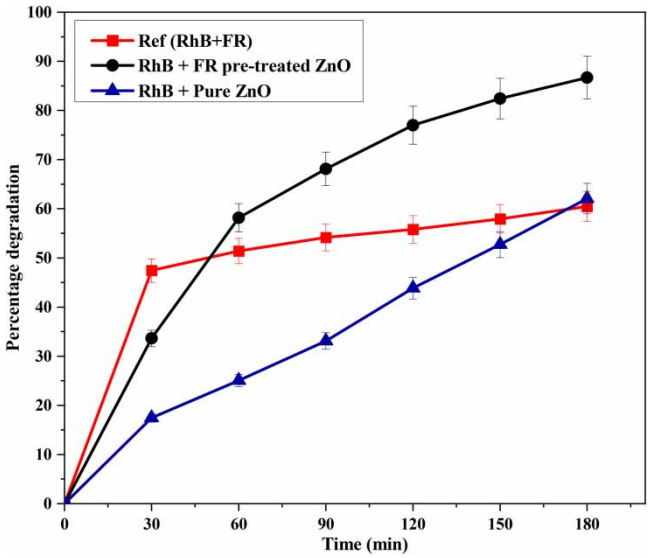

Figure 12 | Effect of pure and FR-pretreated ZnO on the SL degradation of RhB: a comparison. [RhB]: 15 mg/L; [Fe^{2+}/H_2O_2]: [2.5/7.5] mg/L; [ZnO]: 200 mg/L.

The moderate increase in solar degradation of RhB by PS makes it possible to combine PS with other systems (RhB/FR, RhB/FR/ZnO, RhB/ZnO, etc.) in order to accelerate dye degradation. In the presence and absence of ZnO under SL, persulfate leads to an increase in RhB degradation. This might be because, in addition to the presence of $^{\bullet}OH$ radicals from FR, persulfate has the ability to produce the reactive radicals $SO_4^{-\bullet}$ in the presence of SL. As PS concentration rises (from 2.5 to 12.5 mg/L), the oxidizing environment may lead to the formation of increasingly reactive $SO_4^{-\bullet}$ radicals. These radicals can interact with the RhB in water and cause mineralization or destruction of it as in Equation (5) (Brienza & Katsoyiannis 2017; Gayathri *et al.* 2017; Norzaee *et al.* 2017).

$$RhB + SO_4^{-\bullet} \rightarrow \text{Intermediates} \rightarrow SO_4^{2-} + CO_2 + H_2O + \text{salts} \quad (5)$$

When PS is present in greater amounts, $SO_4^{-\bullet}$ can interact with the former to change it into the less reactive $SO_4^{-\bullet}$ as follows (Equation (6)):

$$S_2O_8^{2-} + SO_4^{-\bullet} \rightarrow S_2O_8^{-\bullet} + SO_4^{2-} \quad (6)$$

As a result, the rate of degradation decreases as reaction time improves. The number of reactive free radicals available for the degradation of RhB decreases and the degradation process slows down as the substrate, intermediates, and persulfate compete for the $SO_4^{-\bullet}$. The effect of ZnO on the FR/PS/SL degradation of RhB revealed that ZnO had no influence on the FR/PS-induced degradation at different PS concentrations. ZnO results in the formation of additional $^{\bullet}OH$ radicals. They might, however, be interacting more with the $SO_4^{-\bullet}$, which would cause both to be destroyed by chain termination. As a result, the concentration of $^{\bullet}OH$ and $SO_4^{-\bullet}$ varies over time, causing the degradation to either decrease or stabilize.

It is observed that persulfate emerges as a potential candidate to be used as an alternative oxidant in the photo-Fenton process as it reacts with Fe^{2+} to form sulfate radical ($SO_4^{-\bullet}$) which has a longer lifespan when compared to $^{\bullet}OH$. This could be due to the fact that persulfate has the ability to form reactive radicals $SO_4^{-\bullet}$ in the presence of SL in addition to the presence of $^{\bullet}OH$ radicals from FR. Compared to rates reported for $^{\bullet}OH$, reaction rates between $SO_4^{-\bullet}$, natural organic matter, and ions are slower because $SO_4^{-\bullet}$ only reacts by electron transfer while $^{\bullet}OH$ can react through three separate processes (OH addition, OH reduction, and OH oxidation). As a result, $SO_4^{-\bullet}$ is more stable when treating real matrices with a variety of components. Additionally, by reacting these radicals with hydroxide ions (OH) in FR reagent, $^{\bullet}OH$ may be simultaneously produced in the presence of $SO_4^{-\bullet}$.

Effect of periodic replenishment of FR/FS/HP

One advantage of FR is that pollutant degradation is not prevented by a small reagent excess relative to the stoichiometrically required amount, and the excess reagent can be successfully employed to degrade the fresh substrate (Gayathri *et al.* 2017). Figure 13 shows the impact of the in-between addition of Fe^{2+} (2.5 mg/L), H_2O_2 (7.5 mg/L), and FR (2.5:7.5 (mg/L)), as required to the SF degradation process.

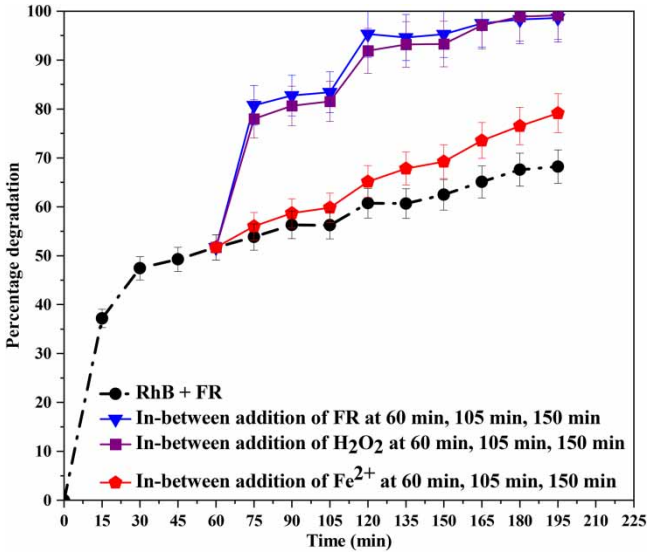

Figure 13 | Effect of 'in between added' FS/HP/FR on SL/FR/RhB degradation. [RhB]: 15 mg/L; [Fe^{2+}/H_2O_2]: [2.5/7.5] mg/L; pH: 3–3.5.

The optimal FS/HP ratio in this case contains an excess of H_2O_2. The addition of Fe^{2+}, when the RhB degradation has stabilized at ~50% only slightly, increases the degradation demonstrating that even under photo-irradiation FS does not become inactive and that the leveling off is not caused by a lack of sufficient FS. The experiments FR and H_2O_2 addition in between further confirm this. In both situations, the degradation is greatly accelerated by the addition of additional reagents at the level-off stages (60 min: 50% degradation; 105 min: 80% degradation). The enhancing effect of the gradual addition of FR and H_2O_2 is diminished with each addition. As a result, adding FR/H_2O_2 after 150 min, when the deterioration is stable at 95%, has no noticeable effect. Since most of the dye has already been degraded at this point, the effect is negligible as there is not enough dye available to fully utilize the FR/H_2O_2 that is already present. This also indicates that in the case of FR, a moderate excess of reagent is always advisable to produce good substrate degradation due to the simultaneous self-decomposition of H_2O_2. Another possibility is that the reactants or intermediaries block the Fe^{2+} or interact ineffectively to produce transient complexes. This aspect requires additional research, which is beyond the focus of this study.

Recycling of Fe^{2+}

As previously mentioned, RhB degrades faster as the concentration of Fe^{2+} increases. Extra ferrous iron does not, however, impact the rate of degradation after a critical optimum. Other researchers also reported comparable observations (Kavitha & Palanivelu 2005; Liu *et al.* 2019; Mahtab *et al.* 2021; Gao *et al.* 2022). The unfavorable loading of dissolved Fe^{2+} in the effluent water with prolonged use of this procedure for water treatment is one of the critiques leveled against the use of the Fenton process for water purification. The rate of degradation accelerated immediately after the addition of extra H_2O_2 (7.5 mg/L) as indicated in Figure 14.

Repeating the cycle (addition of H_2O_2 followed by fresh RhB) several times would confirm that Fe^{2+} could be recycled thereby lowering its excessive loading in the discharged water. As a result, a key objection to the use of FR for water treatment is addressed here. Similar studies have been reported in the context of classic Fenton (Gayathri *et al.* 2016).

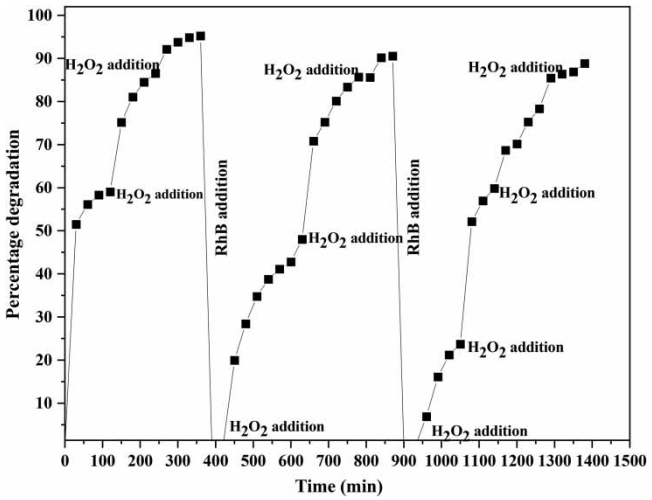

Figure 14 | Recycling of Fe^{2+} in the SL/Fenton process by refilling H_2O_2 periodically. [RhB]: 15 mg/L; [Fe^{2+}:H_2O_2]: (2.5: 7.5) mg/L.

Intermediates analyzed by the LC-MS method

The intermediates identified at 50% degradation of RhB by LC-MS analysis is displayed in Table 1. The precise identification of several of the low molecular weight fragments is not given here. The mass spectral measurements may result in the formation of numerous transitory products, although these are not particularly relevant to the present situation.

Table 1 | List of intermediates detected by LC-MS analysis during SL/FR/RhB degradation

Sl. No.	*m/z*	Intermediates identified during the degradation of RhB
1	443	Rhodamine B (parent compound) 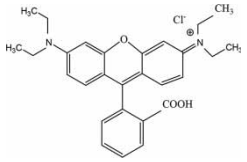
2	431	Hydroxy N-ethyl-N′ ethyl rhodamine 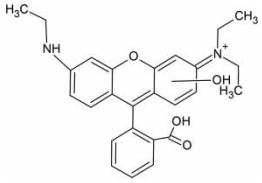
3	415	N,N-diethyl-N′-ethylrhodamine 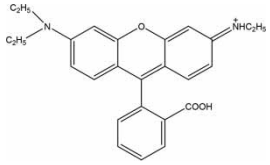
4	403	Hydroxy amino N′ ethyl rhodamine 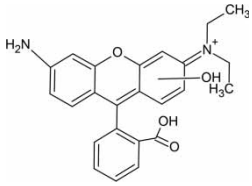

(*Continued.*)

Table 1 | Continued

Sl. No.	*m/z*	Intermediates identified during the degradation of RhB
5	387	N-ethyl-N′-ethylrhodamine 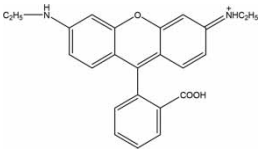
6	359	N-ethyl rhodamine 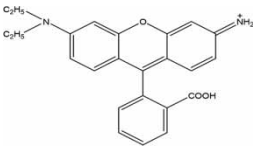
7	359	N-ethylrhodamine 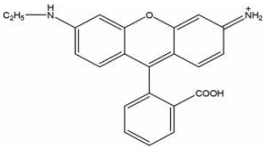
8	138	3-Hydroxybenzoic acid 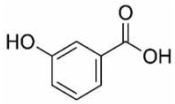
9	117.06	Succinic acid 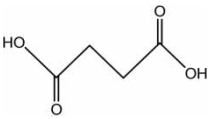
10	91.05	Oxalic acid 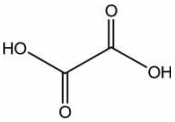

Detection of •OH radicals

The primary mechanism for the degradation of organic pollutants is the production of •OH radicals and other reactive oxygen species, as well as their interactions with substrate molecules. The formation of •OH radicals confirmed by using PL technology (Hoffmann *et al.* 1995; Mohammadi *et al.* 2012; Tijani *et al.* 2022) is given in Figure 15(a) and 15(b). Both systems (with and without ZnO) exhibit a progressive increase in PL intensity at 425 nm during the course of solar irradiation. The concentration of •OH radicals is higher when ZnO is present, proving that the production of more reactive radicals is what drives the degradation of RhB under the SF and solar photocatalytic-Fenton process.

General mechanism of the SL/FR system

The SL/Fenton process has the same basic mechanism as the conventional Fenton process, with the exception that the former is triggered and accelerated by SL. The oxidation of ferrous to ferric ions and the breakdown of H_2O_2 into •OH radicals are the first two steps in the Fenton reaction. Various steps involved in the process are given as follows (Equations (7)–(15)).

$$Fe^{2+} + H_2O_2 \rightarrow Fe^{3+} + {}^{\bullet}OH + OH^{-} \quad (7)$$

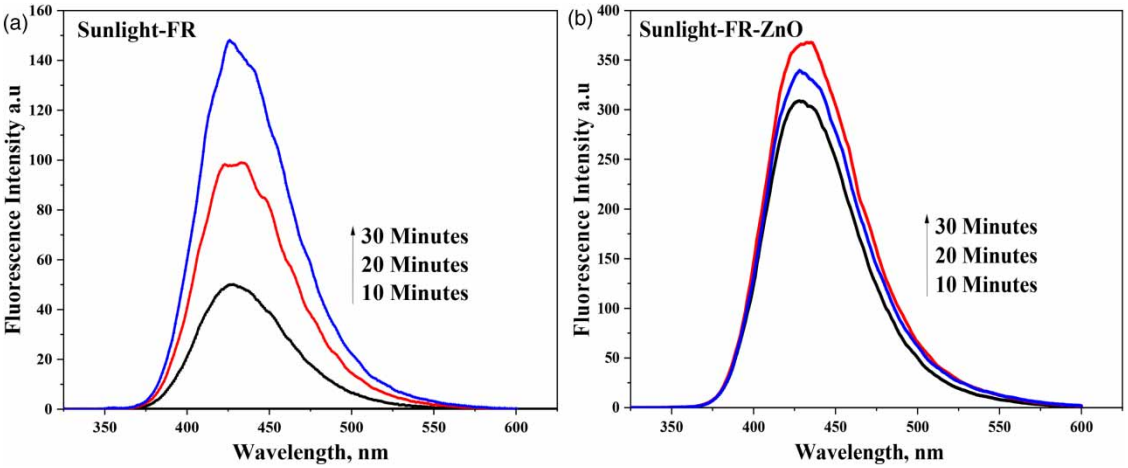

Figure 15 | (a) PL spectrum of the FR/SL system and (b) PL spectrum of the FR/ZnO system.

The Fe^{3+} is reduced by excess H_2O_2 to regenerate Fe^{2+} and form more free radicals as in Equation (8).

$$Fe^{3+} + H_2O_2 \rightarrow Fe^{2+} + H^+ + HO_2^{\bullet} \quad (8)$$

Other possible reactions are:

$$Fe^{2+} + HO_2^{\bullet} \rightarrow Fe^{3+} + HO_2^{\bullet -} \quad (9)$$

$$Fe^{2+} + {}^{\bullet}OH \rightarrow Fe^{3+} + OH^- \quad (10)$$

$$Fe^{3+} + HO_2^{\bullet} \rightarrow Fe^{2+} + O_2 + H^+ \quad (11)$$

The highly reactive free radicals may interact with other radicals, and/or H_2O_2 or may get deactivated by self-scavenging (Equations (12)–(15)).

$${}^{\bullet}OH + {}^{\bullet}OH \rightarrow H_2O_2 \quad (12)$$

$$HO_2^{\bullet} + HO_2^{\bullet} \rightarrow H_2O_2 + O_2 \quad (13)$$

$${}^{\bullet}OH + HO_2^{\bullet} \rightarrow H_2O + O_2 \quad (14)$$

$${}^{\bullet}OH + H_2O_2 \rightarrow HO_2^{\bullet} + H_2O \quad (15)$$

The following reactions also take place when ZnO is present and exposed to light, specifically the UV region of SL, which is approximately 4% of the incident radiation. When ZnO is exposed to solar radiation, electrons are stimulated from its valence band to its conduction band, leaving holes in the former (Equation (16)).

$$ZnO + hv \rightarrow ZnO(e^-) + ZnO(h^+) \quad (16)$$

The holes in the valence band oxidize the OH^- ions that are adsorbed on the surface of the catalyst to $^{\bullet}OH$ radicals (Equation (17)).

$${}^{-}OH + h^+ \rightarrow {}^{\bullet}OH \quad (17)$$

The conduction band electron is transferred to oxygen to create superoxide radical anion $^{\bullet -}O_2$, which subsequently produces additional reactive species like $HO_2^{\bullet}$, $^{\bullet}OH$, H_2O_2, etc. As per the following steps, these species are engaged in photo-oxidation reactions that cause RhB to degrade, eventually mineralize, and produce

H_2O_2 (Equations (18)–(20)).

$$\text{ROS } (^{\bullet}OH, HO_1^{\bullet}, \text{ etc.}) + \text{RhB} \rightarrow \text{Intermediates} + H_2O_2 + H_2O_2 + CO_2 + H_2O \quad (18)$$

$$2^{\bullet}OH \rightarrow H_2O_2 \quad (19)$$

$$HO_2^{\bullet} + HO_2 \rightarrow H_2O_2 + O_2 \quad (20)$$

Under photolysis/photocatalysis, the various other possible reactions are given as follows (Equations (21)–(29)).

$$HO_2^{\bullet} \rightarrow H^+ + O_2^{-\bullet} \quad (21)$$

$$H^+ + O_2^{-\bullet} \rightarrow HO_2^{\bullet} \quad (22)$$

$$[Fe(HO_2)]^{2+} \rightarrow Fe^{2+} + HO_2^{\bullet} \quad (23)$$

$$Fe^{3+} + H_2O_2 \rightarrow e^{2+} + HO_2^{\bullet} + H^+ \quad (24)$$

$$Fe^{2+} + H^+ + O_2^{-\bullet} \rightarrow [Fe(HO_2)]^{2+} \quad (25)$$

$$Fe^{3+} + O_2^{-\bullet} \rightarrow Fe^{2+} + O_2 \quad (26)$$

$$^{\bullet}OH + H_2O_2 \rightarrow H_2O + HO_2^{\bullet} \quad (27)$$

$$2HO_2^{\bullet} \rightarrow H_2O_2 + O_2 \quad (28)$$

$$SO_4^{2-} + H^+ + {}^{\bullet}OH \rightarrow H_2O + SO_4^{-\bullet} \quad (29)$$

The equilibrium reactions possible are as follows (Equations (30)–(35)):

$$Fe^{3+} + HO^- \rightleftharpoons [Fe(OH)]^{2+} \quad (30)$$

$$[Fe(OH)]^{2+} + HO^- \rightleftharpoons [Fe(OH)_2]^+ \quad (31)$$

$$[Fe(SO_4)]^+ \rightleftharpoons Fe^{3+} + SO_4^{2-} \quad (32)$$

$$SO_4^{2-} + H^+ \rightleftharpoons HSO_4^- \quad (33)$$

$$Fe^{3+} + H_2O_2 \rightleftharpoons [Fe(HO_2)]^{2+} + H^+ \quad (34)$$

$$[Fe(OH)]^{2+} + H_2O_2 \rightleftharpoons [Fe(OH)(HO_2)]^+ + H^+ \quad (35)$$

H_2O_2 self-decomposes and becomes deactivated in the absence of any organic substrate to be oxidized, as in Equation (36):

$$2H_2O_2 \rightarrow 2H_2O + O_2 \quad (36)$$

Various other reactions that can occur in the presence of RhB are listed in reactions (37)–(39). RhB is represented as R.

$$^{\bullet}OH + R \rightarrow H_2O + R^{\bullet} \rightarrow (\text{Partial mineralization} + \text{Colorless intermediates}) \quad (37)$$

$$R^{\bullet} + Fe^{2+} \rightarrow R^- + Fe^{3+} \quad (38)$$

$$R^{\bullet} + Fe^{3+} \rightarrow R^+ + Fe^{2+} \quad (39)$$

The free radical R$^{\bullet}$ undergoes dimerization as well as in Equation (40).

$$R^{\bullet} + R^{\bullet} \rightarrow RR \quad (40)$$

Mineralization takes place eventually as in (41).

$$R^{\bullet} \text{ or } R^{-} \text{ or } R^{+} \text{ or } RR + {}^{\bullet}OH,\ HO_2^{\bullet},\ H_2O_2 \text{ etc.} \rightarrow \text{intermediates} \rightarrow CO_2 + H_2O + \text{salts (mineralization)} \quad (41)$$

Many of the above mentioned reactive free radicals are produced by the Fenton process even in ambient conditions, i.e., conventional Fenton. They can generate intermediates and finally mineralize the pollutant by interacting with RhB in a number of ways. The decomposition and mineralization processes can be accelerated when solar energy is used as an external energy source. When ZnO, which functions as an effective photocatalyst, under UV/visible light (SL) is present, the degradation is further accelerated. Based on the results of the current study, it is seen that the SF process and solar photocatalytic-Fenton process significantly enhance the efficiency of the conventional Fenton process for the degradation and mineralization of RhB.

CONCLUSION

The work demonstrates that the traditional Fenton reaction, which uses H_2O_2 and a simple ferrous salt at ambient conditions, may be revisited and used as a powerful advanced oxidation technology to remove hazardous contaminants from water. Fenton reaction is a convenient option for cost-effective and efficient wastewater treatment due to the relative simplicity of the procedure. The RhB dye is used as a model pollutant to illustrate the efficiency of the Fenton process for complete degradation and mineralization under SL. Solar activation improves the efficiency of the classic Fenton process for purifying water from dye contamination. Mineralization is successfully completed using ZnO as the catalyst and SL as the activation source. It also reports the difference in the behavior of ZnO in classic Fenton and solar photocatalytic-Fenton. By recycling the Fenton sludge and replenishing the used-up H_2O_2 regularly, the drawbacks of accumulation of Fe^{2+}/Fe^{3+} can be eliminated. During the process itself, the Fe^{2+} that is converted into Fe^{3+} is converted back to Fe^{2+}. FS/HP ratio and pH are crucial for maximizing efficiency. By using LC-MS analysis, several intermediates formed during the degradation are identified. The effectiveness of the solar photocatalytic Fenton process for treating wastewater economically is demonstrated here. Solar energy is a natural, inexhaustible, and renewable source of energy. Thus, as a green and efficient degradation technology, SL/FR/ZnO is favored for its advantages of high removal rate, short time use, wide concentration range, low cost, good stability, and no secondary pollution.

ACKNOWLEDGEMENTS

Financial support from the University Grants Commission (UGC), India, is gratefully acknowledged by way of the Senior Research Fellowship to P.V.G. The authors would like to thank Kerala University of Fisheries and Ocean Studies (KUFOS), St. Albert's College, and Cochin University of Science and Technology (CUSAT) for providing the necessary laboratory facilities, equipment, materials, etc. to conduct the study. The authors also thank two anonymous reviewers for their constructive evaluation of our manuscript, which significantly enhanced the overall quality of the manuscript.

AUTHORS' CONTRIBUTIONS

P.V.G. conceived the idea, conducted the research work, and wrote the manuscript. S.J. reviewed and edited the manuscript and conducted overall supervision of the work. E.P.Y. designed the study, and reviewed and edited the manuscript. S.Y. supported the experimental setup and reviewed the manuscript. All authors read and approved the final manuscript.

FUNDING

The first author was supported by the University Grants Commission (UGC), India by way of a Senior Research Fellowship, and Kerala University of Fisheries and Ocean Studies (KUFOS) by way of a Post-Doctoral Fellowship.

ETHICS APPROVAL

All ethics were followed during the preparation of the manuscript. Unethical actions were not made.

CONSENT TO PARTICIPATE

All authors gave consent to participate in this publication.

CONSENT FOR PUBLICATION

All authors gave consent for publication in the journal *Water Practice and Technology*.

DATA AVAILABILITY STATEMENT

All relevant data are included in the paper or its Supplementary Information.

CONFLICT OF INTEREST

The authors declare there is no conflict.

REFERENCES

Ameta, S. C. & Ameta, R. 2018 *Advanced Oxidation Processes for Wastewater Treatment: Emerging Green Chemical Technology*. Academic press, 125 London Wall, London EC 2Y 5AS, UK.

Andreozzi, R., Caprio, V., Insola, A. & Marotta, R. 1999 Advanced oxidation processes (AOP) for water purification and recovery. *Catalysis Today* **53**(1), 51–59. https://doi.org/10.1016/S0920-5861(99)00102-9.

Anju, S., Jyothi, K., Joseph, S. S. & Yesodharan, E. P. 2012 Ultrasound-assisted semiconductor mediated catalytic degradation of organic pollutants in water: comparative efficacy of ZnO, TiO_2 and ZnO–TiO_2. *Research Journal of Recent Sciences* **2277**, 2502.

Asgari, E., Aghanaghad, M., Nourmoradi, H., Hashemzadeh, B. & Aali, R. 2020 Biodegradability enhancement and pre-treatment of industrial estate wastewater by the electro-Fenton process. *Desalination and Water Treatment* **200**, 217–223. https://doi.org/10.5004/dwt.2020.26132.

Babuponnusami, A. & Muthukumar, K. 2011 Degradation of phenol in aqueous solution by fenton, sono-fenton and sono-photo-fenton methods. *Clean–Soil, Air, Water* **39**(2), 142–147. https://doi.org/10.1002/clen.201000072.

Brienza, M. & Katsoyiannis, I. A. 2017 Sulfate radical technologies as tertiary treatment for the removal of emerging contaminants from wastewater. *Sustainability* **9**(9), 1604. https://doi.org/10.3390/su9091604.

Çalık, Ç. & Çifçi, D. İ. 2022 Comparison of kinetics and costs of Fenton and photo-Fenton processes used for the treatment of textile industry wastewater. *Journal of Environmental Management* **304**:114234. https://doi.org/10.1016/j.jenvman.2021.114234.

Costa, R. C., Moura, F. C., Ardisson, J. D., Fabris, J. D. & Lago, R. M. 2008 Highly active heterogeneous Fenton-like systems based on Fe0/Fe3O4 composites prepared by controlled reduction of iron oxides. *Applied Catalysis B* **83**(1–2), 131–139. https://doi.org/10.1016/j.apcatb.2008.01.039.

Diao, Z. H., Xu, X. R., Jiang, D., Li, G., Liu, J. J., Kong, L. J. & Zuo, L. Z. 2017 Enhanced catalytic degradation of ciprofloxacin with fes2/SiO_2 microspheres as heterogeneous Fenton catalyst: kinetics, reaction pathways, and mechanism. *Journal of Hazardous Materials* **327**, 108–115. https://doi.org/10.1016/j.jhazmat.2016.12.045.

Du, H., Zhang, Y., Jiang, H. & Wang, H. 2022 Adsorption of rhodamine B on polyvinyl chloride, polystyrene, and polyethylene terephthalate microplastics in aqueous environments. *Environmental Technology & Innovation* **27**, 102495.

Eaton, A. D., Clesceri, L. S., Rice, E. W. & Greenberg, A. E. 2005 *Standard Methods for the Examination of Water and Wastewater*. American public health association, Washington, pp. 515–516.

Egbosiuba, T. C., Abdulkareem, A. S., Kovo, A. S., Afolabi, E. A., Tijani, J. O., Auta, M. & Roos, W. D. 2020 Ultrasonic enhanced adsorption of methylene blue onto the optimized surface area of activated carbon: adsorption isotherm, kinetics, and thermodynamics. *Chemical Engineering Research and Design* **153**, 315–336.

Elmobarak, W. F., Hameed, B. H., Almomani, F. & Abdullah, A. Z. 2021 A review on the treatment of petroleum refinery wastewater using advanced oxidation processes. *Catalysts* **11**(7), 782. https://doi.org/10.3390/catal11070782.

Furia, F., Minella, M., Gosetti, F., Turci, F., Sabatino, R., Di Cesare, A., Corno, G. & Vione, D. 2021 Elimination from wastewater of antibiotics reserved for hospital settings, with a Fenton process based on zero-valent iron. *Chemosphere* **283**, 131170. https://doi.org/10.1016/j.chemosphere.2021.131170.

Gao, L., Cao, Y., Wang, L. & Li, S. 2022 A review on sustainable reuse applications of Fenton sludge during wastewater treatment. *Frontiers of Environmental Science & Engineering* **16**(6), 1–12. https://doi.org/10.1007/s11783-021-1511-6.

Gayathri, P. V., Yesodharan, E. P. & Suguna, Y. 2016 Investigations on classic Fenton reaction as a simple inexpensive technique for the removal of toxic chemical pollutants from water. *Indian Journal of Applied Research* **6**(8), 28–33.

Gayathri, P. V., Suguna, Y. & Yesodharan, E. P. 2017 Purification of water contaminated with traces of Rhodamine B dye by microwave-assisted, oxidant-induced and zinc oxide catalyzed advanced oxidation process. *Desalination and Water Treatment* **85**, 161–174. 10.5004/dwt.2017.21286.

Gayathri, P. V., Suguna, Y. & Yesodharan, E. P. 2019 Microwave/Persulphate assisted ZnO mediated photocatalysis (MW/PS/UV/ZnO) as an efficient advanced oxidation process for the removal of RhB dye pollutant from water. *Journal of Environmental Chemical Engineering* **7**(4), 103122. https://doi.org/10.1016/j.jece.2019.103122.

Ghosh, P., Samanta, A. N. & Ray, S. 2010 COD reduction of petrochemical industry wastewater using Fenton's oxidation. *The Canadian Journal of Chemical Engineering* **88**(6), 1021–1026. https://doi.org/10.1002/cjce.20353.

Gou, Y., Chen, P., Yang, L., Li, S., Peng, L., Song, S. & Xu, Y. 2021 Degradation of fluoroquinolones in homogeneous and heterogeneous photo-Fenton processes: a review. *Chemosphere* **270**, 129481. https://doi.org/10.1016/j.chemosphere.2020.129481.

Gulkaya, I., Surucu, G. A. & Dilek, F. B. 2006 Importance of H_2O_2/Fe^{2+} ratio in Fenton's treatment of a carpet dyeing wastewater. *Journal of Hazardous Materials* **136**(3), 763–769. https://doi.org/10.1016/j.jhazmat.2006.01.006.

He, J., Yang, X., Men, B. & Wang, D. 2016 Interfacial mechanisms of heterogeneous Fenton reactions catalyzed by iron-based materials: a review. *Journal of Environmental Sciences* **39**, 97–109. https://doi.org/10.1016/j.jes.2015.12.003.

Hoffmann, M. R., Martin, S. T., Choi, W. & Bahnemann, D. W. 1995 Environmental applications of semiconductor photocatalysis. *Chemical Reviews* **95**(1), 69–96. https://doi.org/10.1021/cr00033a004.

Jain, S., Yamgar, R. & Jayaram, R. V. 2009 Photolytic and photocatalytic degradation of atrazine in the presence of activated carbon. *Chemical Engineering Journal* **148**(2–3), 342–347. https://doi.org/10.1016/j.cej.2008.09.006.

Jyothi, K. P., Yesodharan, S. & Yesodharan, E. P. 2014 Ultrasound (US), ultraviolet light (UV) and combination (US+ UV) assisted semiconductor catalyzed degradation of organic pollutants in water: oscillation in the concentration of hydrogen peroxide formed in situ. *Ultrasonic Sonochemistry* **21**(5), 1787–1796. https://doi.org/10.1016/j.ultsonch.2014.03.019.

Kavitha, V. & Palanivelu, K. 2005 Destruction of cresols by Fenton oxidation process. *Water Research* **39**(13), 3062–3072. https://doi.org/10.1016/j.watres.2005.05.011.

Khare, P., Patel, R. K., Sharan, S. & Shankar, R. 2021 Recent trends in advanced oxidation process for treatment of recalcitrant industrial effluents. *Advanced Oxidation Processes for Effluent Treatment Plants* 137–160. https://doi.org/10.1016/B978-0-12-821011-6.00008-6.

Kondamareddy, K. K., Bin, H., Lu, D., Kumar, P., Dwivedi, R. K., Pelenovich, V. O., Zhao, X. Z., Gao, W. & Fu, D. 2018 Enhanced visible light photodegradation activity of RhB/MB from aqueous solution using nanosized novel Fe-Cd co-modified ZnO. *Scientific Reports* **8**(1), 1–12. https://doi.org/10.1038/s41598-018-29025-1.

Li, D., Zheng, T., Yu, J., He, H., Shi, W. & Ma, J. 2022 Enhancement of the electro-Fenton degradation of organic contaminant by accelerating Fe^{3+}/Fe^{2+} cycle using hydroxylamine. *Journal of Industrial and Engineering Chemistry* **105**, 405–413. https://doi.org/10.1016/j.jiec.2021.09.041.

Liu, L., Liu, S., Mishra, S. B. & Sheng, L. 2019 An easily applicable and recyclable Fenton-like catalyst produced without wastewater emission and its performance evaluation. *Journal of Cleaner Production* 234653–234659. https://doi.org/10.1016/j.jclepro.2019.06.230.

Lu, M. 2013 *Photocatalysis and Water Purification: From Fundamentals to Recent Applications*. John Wiley-VCH, Verlag GmbH & Co. KGaA, Boschstr.12, 69469 Wienheim, Germany.

Luo, H., Zeng, Y., He, D. & Pan, X. 2021 Application of iron-based materials in heterogeneous advanced oxidation processes for wastewater treatment: a review. *Chemical Engineering Journal* **407**, 127191. https://doi.org/10.1016/j.cej.2020.127191.

Mahtab, M. S., Farooqi, I. H. & Khursheed, A. 2021 Zero Fenton sludge discharge: a review on reuse approach during wastewater treatment by the advanced oxidation process. *International Journal of Environmental Science and Technology* 1–14. https://doi.org/10.1007/s13762-020-03121-0.

Maroudas, A., Pandis, P. K., Chatzopoulou, A., Davellas, L. R., Sourkouni, G. & Argirusis, C. 2021 Synergetic decolorization of azo dyes using ultrasounds, photocatalysis and photo-fenton reaction. *Ultrasonic Sonochemistry* **71**, 105367. https://doi.org/10.1016/j.ultsonch.2020.105367.

Mei, L., Peng, C., Qiao, H., Ke, F., Liang, J., Hou, R., Wan, X. & Cai, H. 2019 Enhanced removal of fluoride by zirconium modified tea waste with extrusion treatment: kinetics and mechanism. *RSC Advances* **9**(57), 33345–33353. https://doi.org/10.1039/C9RA07155E.

Mohammadi, A. S., Asgari, G., Ebrahimi, A., Sharifi, Z. & Attar, H. M. 2012 4-Chlorophenol degradation with modified domestic microwave and hydrogen peroxide in aqueous solution. *International Journal of Environmental Health Engineering* **1**(1), 46. 10.4103/2277-9183.105345.

Ndamitso, M. M., Abdulkareem, A. S. & Tijani, J. O. 2020 Application of TiO_2 and ZnO nanoparticles immobilized on clay in wastewater treatment: a review. *Applied Water Science* **10**, 49. https://doi.org/10.1007/s13201-019-1138-y.

Norzaee, S., Bazrafshan, E., Djahed, B., Kord Mostafapour, F. & Khaksefidi, R. 2017 UV activation of persulfate for removal of penicillin G antibiotics in aqueous solution. *The Scientific World Journal* **3519487**, 6. https://doi.org/10.1155/2017/3519487.

Onu, D. C., Babayemi, A. K., Egbosiuba, T. C., Okafor, B. O., Ani, I. J., Mustapha, S., Tijani, J. O., Ulakpa, W. C., Ovuoraye, P. E. & Abdulkareem, A. S. 2023 Isotherm, kinetics, thermodynamics, recyclability and mechanism of ultrasonic assisted adsorption of methylene blue and lead (II) ions using green synthesized nickel oxide nanoparticles. *Environmental Nanotechnology, Monitoring & Management* **20**, 100818.

Pandey, S., Mandari, K. K., Kim, J., Kang, M. & Fosso-Kankeu, E. 2020 Recent advancement in visible-light-responsive photocatalysts in heterogeneous photocatalytic water treatment technology. *Photocatalysts in Advanced Oxidation Processes for Wastewater treatment* 167–196. https://doi.org/10.1002/9781119631422.ch6.

Pouran, S. R., Aziz, A. A. & Daud, W. M. A. W. 2015 Review on the main advances in photo-Fenton oxidation system for recalcitrant wastewaters. *Journal of Industrial and Engineering Chemistry* **21**, 53–69. https://doi.org/10.1016/j.jiec.2014.05.005.

Saeed, M., Muneer, M. & Akram, N. 2021 Photocatalysis: an effective tool for photodegradation of dyes-a review. *Environmental Science and Pollution Research* **29**, 293–311. https://doi.org/10.1007/s11356-021-16389-7.

Sannino, D., Vaiano, V., Isupova, L. A. & Ciambelli, P. 2012 Heterogeneous photo-Fenton oxidation of organic pollutants on structured catalysts. *Journal of Advanced Oxidation Technology* **15**(2), 294–300. https://doi.org/10.1515/jaots-2012-0207.

Sayed, M., Pingfeng, F., Khan, H. M. & Zhang, P. 2014 Effect of isopropanol on microstructure and activity of TiO_2 films with dominant {001} facets for photocatalytic degradation of bezafibrate. *International Journal of Photoenergy* **2014**, 490264. https://doi.org/10.1155/2014/490264.

Scaria, J., Gopinath, A. & Nidheesh, P. V. 2021 A versatile strategy to eliminate emerging contaminants from the aqueous environment: heterogeneous Fenton process. *Journal of Cleaner Production* **278**, 124014. https://doi.org/10.1016/j.jclepro.2020.124014.

Shah, N. S., Iqbal, J., Sayed, M., Ghfar, A. A., Khan, J. A., Khan, Z. U. H., Murtaza, B., Boczkaj, G. & Jamil, F. 2022 Enhanced solar light photocatalytic performance of Fe-ZnO in the presence of H_2O_2, $S_2O_8^{2-}$, and HSO_5^- for degradation of chlorpyrifos from agricultural wastes: toxicities investigation. *Chemosphere* **287**, 132331. https://doi.org/10.1016/j.chemosphere.2021.132331.

Sivakumar, S., Selvaraj, A., Ramasamy, A. K. & Balasubramanian, V. 2013 Enhanced photocatalytic degradation of reactive dyes over $FeTiO_3/TiO_2$ heterojunction in the presence of H_2O_2. *Water, Air, & Soil Pollution* **224**(5), 1–13. https://doi.org/10.1007/s11270-013-1529-x.

Suty, H., De Traversay, C. & Cost, M. 2004 Applications of advanced oxidation processes: present and future. *Water Science and Technology* **49**(4), 227–233. https://doi.org/10.2166/wst.2004.0270.

Tang, Z., Zhao, P., Wang, H., Liu, Y. & Bu, W. 2021 Biomedicine meets Fenton chemistry. *Chemical Reviews* **121**(4), 1981–2019. https://doi.org/10.1021/acs.chemrev.0c00977.

Tijani, J. O., Odeh, E. I., Mustapha, S., Egbosiuba, T. C., Daniel, A. I., Abdulkareem, A. S. & Muya, F. N. 2022 Photocatalytic, electrochemical, antibacterial and antioxidant behaviour of carbon-sulphur Co-doped zirconium (IV) oxide nanocomposite. *Cleaner Chemical Engineering* **3**, 100034.

Uko, C. A., Tijani, J. O., Abdulkareem, S. A., Mustapha, S., Egbosiuba, T. C. & Muzenda, E. 2022 Adsorptive properties of MgO/WO3 nano adsorbent for selected heavy metals removal from indigenous dyeing wastewater. *Process Safety and Environmental Protection* **162**, 775–794.

Veena, V., Suguna, Y. & Yesodharan, E. P. 2019 Significant enhancement in the efficiency of the Fenton process by solar, electrolytic and sonolytic activation for the mineralization of indigo carmine Dye pollutant in water. *American Journal of Engineering Research* **8**(6), 135–154.

Venâncio, J. P., Rodrigues, C. S., Nunes, O. C. & Madeira, L. M. 2022 Application of iron-activated persulfate for municipal wastewater disinfection. *Journal of Hazardous Materials* **426**, 127989. https://doi.org/10.1016/j.jhazmat.2021.127989.

Vilela, P. B., Martins, A. S., Starling, M. C. V., de Souza, F. A., Pires, G. F., Aguilar, A. P., Pinto, M. E. A., Mendes, T. A. & de Amorim, C. C. 2021 Solar photon-Fenton process eliminates free plasmid DNA harboring antimicrobial resistance genes from wastewater. *Journal of Environmental Management* **285**, 112204. https://doi.org/10.1016/j.jenvman.2021.112204.

Xia, H., Li, C., Yang, G., Shi, Z., Jin, C., He, W., Xu, J. & Li, G. 2022 A review of microwave-assisted advanced oxidation processes for wastewater treatment. *Chemosphere* **287**, 131981. https://doi.org/10.1016/j.chemosphere.2021.131981.

Yu, D. & Pei, Y. 2021 Removal of ibuprofen by sodium alginate–coated iron-carbon granules combined with the ultrasound and Fenton technologies: influencing factors and degradation intermediates. *Environmental Science and Pollution Research* **28**(17), 21183–21192. https://doi.org/10.1007/s11356-020-10455-2.

Zaidi, R., Khan, S. U., Farooqi, I. H. & Azam, A. 2021 Investigation of kinetics and adsorption isotherm for fluoride removal from aqueous solutions using mesoporous cerium–aluminum binary oxide nanomaterials. *RSC Advances* **11**(46), 28744–28760. https://doi.org/10.1039/D1RA00598G.

First received 26 April 2023; accepted in revised form 19 July 2023. Available online 1 August 2023